## Response to Editor

We thank the editor for the robust examination of our paper and useful comments.

*Comments to the Author:*
*Thank you for addressing the issues raised.*

*I have some minor comments below, all about wording.*

*46 …estimate the magnitude…*
*53 you might want to add a reference to the recent paper by Hmiel et a (https://doi.org/10.1038/s41586-020-1991-8 ).*
*149 …that, based on the EPA gridded inventory (Maasakkers et al, 2016), increase…*
*170 Wind speed and direction were measured…*
*273ff Temporal variability in what? Background concentration, emission?? Do not write much but do clarify.*
*337 Inventory*
*422 …using the INFLUX network, we estimate that… (2 changes)*
*444 …features in Figure 7 is a …*
*512 ….methods. The atmospheric inverse flux….. (Could be Our atmospheric….)*

All of the comments above were addressed to the best of our ability (see the updated combined document).

# Background Heterogeneity and Other Uncertainties in Estimating Urban Methane Flux: Results from the Indianapolis Flux (INFLUX) Experiment

Nikolay V. Balashov[1*,2,3], Kenneth J. Davis[1], Natasha L. Miles[1], Thomas Lauvaux[1,4], Scott J. Richardson[1], Zachary R. Barkley[1], Timothy A. Bonin[5, 6]

[1]The Pennsylvania State University, University Park, Pennsylvania, USA
[2]NASA Postdoctoral Program, Universities Space Research Association, 7178 Columbia Gateway Drive, Columbia, MD, 21046, USA
[3]NASA Global Modeling and Assimilation Office (GMAO), Goddard Space Flight Center, Greenbelt, MD, 20771, USA
[4]Laboratory of Climate Sciences and Environment, Gif-sur-Yvette, France
[5]Cooperative Institute for Research in Environmental Sciences, Boulder, Colorado, USA
[6]Chemical Sciences Division, National Oceanic and Atmospheric Administration, Boulder, Colorado, USA
[*]Former affiliation

*Correspondence to*: Nikolay V. Balashov (nvb5011@psu.edu or nikolay.v.balashov@nasa.gov) and Kenneth J. Davis (kjd10@psu.edu)

**Abstract**

As natural gas extraction and use continues to increase, the need to quantify emissions of methane ($CH_4$), a powerful greenhouse gas, has grown. Large discrepancies in Indianapolis $CH_4$ emissions have been observed when comparing inventory, aircraft mass-balance, and tower inverse modeling estimates. Four years of continuous $CH_4$ mole fraction observations from a network of nine towers as a part of the Indianapolis Flux Experiment (INFLUX) are utilized to investigate four possible reasons for the abovementioned inconsistencies: (1) differences in definition of the city domain, (2) a highly temporally variable and spatially non-uniform $CH_4$ background, (3) temporal variability in $CH_4$ emissions, and (4) $CH_4$ sources that are not accounted for in the inventory. Reducing the Indianapolis urban domain size to be consistent with the inventory domain size decreases the $CH_4$ emission estimation of the inverse modeling methodology by about 35%, thereby lessening the discrepancy and bringing total city flux within the error range of one of the two inventories. Nevertheless, the inverse modeling estimate still

remains about 91% higher than inventory estimates. Hourly urban background $CH_4$ mole fractions are shown to be spatially heterogeneous and temporally variable. Variability in background mole fractions observed at any given moment and a single location could be up to about 50 ppb depending on a wind direction, but decreases substantially when averaged over multiple days. Statistically significant, long-term biases in background mole fractions of 2-5 ppb are found from single point observations for most wind directions. Boundary layer budget estimates suggest that Indianapolis $CH_4$ emissions did not change significantly when comparing 2014 to 2016. However, it appears that $CH_4$ emissions may follow a diurnal cycle with daytime emissions (12-16 LST) approximately twice as large as nighttime emissions (20-5 LST). We found no evidence for large $CH_4$ point sources that are otherwise missing from the inventories. The data from the towers confirm that the strongest $CH_4$ source in Indianapolis is South Side Landfill. Leaks from the natural gas distribution system that were detected with the tower network appeared localized and non-permanent. Our simple atmospheric budget analyses estimate the magnitude of the diffuse NG source to be 70% higher than inventory estimates, but more comprehensive analyses are needed. Long-term averaging, spatially-extensive upwind mole fraction observations, mesoscale atmospheric modeling of the regional emissions environment, and careful treatment of the times of day are recommended for precise and accurate quantification of urban $CH_4$ emissions.

## 1 Introduction

From the beginning of the Industrial Revolution to 2011, atmospheric methane ($CH_4$) mole fractions increased by a factor of 2.5 due to anthropogenic processes such as fossil fuel production, waste management, and agricultural activities (Ciais et al., 2013; Hmiel et al., 2020).

The increase in $CH_4$ is a concern as it is a potent greenhouse gas (GHG) with a global warming potential 28-34 times greater than that of $CO_2$ over a period of 100 years (Myhre et al., 2013). The magnitudes of component $CH_4$ sources, and the causes of variability in the global $CH_4$ budget are not well understood with theories attributing changes in biogenic, thermogenic, and pyrogenic emissions or a decline in the atmospheric $CH_4$ sink to the recent $CH_4$ increases (Nisbet et al., 2016; Saunois et al., 2016; Nisbet et al., 2019; Hmiel et al., 2020). Improved understanding of $CH_4$ emissions is needed (National Academies of Sciences and Medicine, 2018).

In particular, the estimates of continental U.S. anthropogenic $CH_4$ emissions disagree. Inventories from Environment Protection Agency (EPA) and Emissions Database for Global Atmospheric Research (EDGAR) in 2008 reported emission values of 19.6 and 22.1 TgC $y^{-1}$ (U.S. EPA, 2013; European Commission Joint Research Centre and Netherlands Environmental Assessment Agency, 2010). However, top-down methodologies using aircraft and inverse modeling framework found emission values of 32.4 ± 4.5 TgC $y^{-1}$ for 2004 and 33.4 ± 1.4 TgC $y^{-1}$ for 2007-2008 respectively (Kort et al., 2008; Miller et al., 2013). Underestimation of natural gas (NG) production and agricultural sources are possible reasons for this disagreement (Miller et al., 2013; Brandt et al., 2014; Jeong et al., 2014). Efforts to reconcile GHGs emissions estimates using atmospheric methods and inventory assessment have sometimes succeeded (Schuh et al., 2013; Zavala-Araiza et al., 2015; Turnbull et al., 2019) when careful attention is given to the details of each method, and targeted atmospheric data are available. A recent synthesis of emissions from the U.S. NG supply chain demonstrated similar success and concluded that current inventory estimates of emissions from U.S. NG production are too low

Nikolai Balashov 3/10/2020 3:54 PM
**Deleted:** although there is some evidence that

Nikolai Balashov 3/11/2020 5:48 PM
**Deleted:**

Nikolai Balashov 3/10/2020 3:56 PM
**Deleted:** may play an important role in

Nikolai Balashov 3/10/2020 3:59 PM
**Formatted:** Subscript

118 and that emission from NG distribution is one of the greatest remaining sources of uncertainty in
119 the NG supply chain (Alvarez et al., 2018).

120 Due to the uncertainties in $CH_4$ emissions from NG distribution it is natural that urban
121 emissions are of interest as well. For example, two studies (McKain et al., 2015; Hendrick et al.,
122 2016) indicate that ~60-100% of Boston $CH_4$ emissions are attributable to the NG distribution
123 system. Recent studies of urban $CH_4$ emissions in California indicate that the California Air
124 Resources Board (CARB) inventory tends to underestimate the actual $CH_4$ urban fluxes possibly
125 due to fugitive emissions from NG infrastructures in urban environments (Wunch et al., 2009;
126 Jeong et al., 2016; Jeong et al., 2017). The accuracy and precision of atmospheric estimates of
127 urban $CH_4$ emissions are limited by available atmospheric observations (Townsend-Small et al.,
128 2012), potential source magnitude variability with time (Jackson et al., 2014; Lamb et al., 2016),
129 errors in atmospheric transport modeling (Hendrick et al., 2016; Deng et al., 2017; Sarmiento et
130 al., 2017), and complexity in atmospheric background conditions (Cambaliza et al., 2014; Karion
131 et al., 2015; Heimburger et al., 2017). In this work, detailed analysis of urban $CH_4$ mole
132 fractions is performed for the city of Indianapolis to better understand the aforementioned
133 uncertainties of urban $CH_4$ emissions.

134 The Indianapolis Flux Experiment (INFLUX; Davis et al., 2017) is a testbed for
135 improving quantification of urban GHGs emissions and their variability in space and time.
136 INFLUX (http://influx.psu.edu) is located in Indianapolis partly because of its isolation from
137 other urban centers and the flat Midwestern terrain. It includes a very dense GHGs monitoring
138 network, comprised of irregular insitu aircraft measurements (Heimburger et al., 2017;
139 Cambaliza et al., 2014), continuous in situ observations from communications towers using
140 cavity ring-down spectroscopy (Richardson et al., 2017; Miles et al., 2017), and automated flask

141 sampling systems for quantification of a wide variety of trace gases (Turnbull et al., 2015).
142 Meteorological sensors include a Doppler lidar providing continuous boundary layer depth and
143 wind profiles, and tower-based eddy covariance measurements of the fluxes of momentum,
144 sensible and latent heat (Sarmiento et al., 2017). The network is designed for emissions
145 quantification using top-down methods such as tower-based inverse modeling (Lauvaux et al.,
146 2016) and aircraft mass balance estimates (Cambaliza et al., 2015).

147 Lamb et al. (2016) compared Indianapolis $CH_4$ emissions estimates from a variety of
148 approaches, specifically inventory, aircraft mass balances, and inverse modeling. The results
149 revealed large mean differences among the city fluxes estimated from these methods (Fig. 1). In
150 general, the inventory methods arrived at lower estimates of emissions compared to the
151 atmospheric, or top-down approaches. $CH_4$ fluxes calculated using the aircraft mass balance
152 technique varied considerably between flights, more than would be expected from propagation of
153 errors of the component measurements (Cambaliza et al., 2014; Lamb et al., 2016). The
154 atmospheric inverse estimate was significantly higher than the inventory and some of the
155 aircraft-derived values.

156 Biogenic emissions from the city are dominated by a landfill close to downtown, and
157 these emissions are thought to be fairly well known (GHG reporting program). Although
158 evidence of possible variability in landfill emissions exists from Cambaliza et al. (2015), which
159 used aircraft mass balance on five different occasions to calculate $CH_4$ flux from this landfill.
160 Uncertainty in total city emissions is mainly driven by the uncertainty in thermogenic emissions,
161 which are hypothesized to emerge largely from the NG distribution system (Mays et al., 2009;
162 Cambaliza et al., 2015; Lamb et al., 2016). In this study, we explore potential explanations for

the discrepancies in $CH_4$ emissions estimates from Indianapolis and posit methods and recommendations for the study of $CH_4$ emissions from other urban centers.

We examine four different potential explanations for the $CH_4$ flux discrepancies reported in Lamb et al. (2016): (1) inconsistent geographic boundaries between top-down and bottom-up studies, (2) heterogeneity in the urban scale $CH_4$ background and (3) temporal variability in urban emissions, which is not captured by the existing top-down studies, and (4) $CH_4$ sources that are not accounted for in the inventories. Well-calibrated $CH_4$ sensors on the INFLUX tower network (Miles et al., 2017) collected continuous $CH_4$ observations from 2013 to 2016 and provide a unique opportunity to explore these issues.

## 2 Methods

### 2.1 Experimental site

This study uses data from a tower-based GHG observational network located in the city and surrounding suburbs of Indianapolis, Indiana in the Midwestern U.S. Prior studies have used varying definitions for the region of Indianapolis (Cambaliza et al., 2015; Lamb et al., 2016). In this work, we follow Gurney et al. (2012) and define Indianapolis as the area of Marion County. The flat terrain of the region simplifies interpretation of the atmospheric transport. The land-surface heterogeneity inherent in the urban environment (building roughness, spatial variations in the surface energy balance) does have a modest influence on the wind and boundary layer depth within the city compared to nearby rural areas (Sarmiento et al., 2017).

Figure 2 shows two domains that have been used for the evaluation of Indianapolis $CH_4$ emissions (Lamb et al., 2016; Lauvaux et al., 2016). The first domain is the whole area shown in

Nikolai Balashov 3/11/2020 6:03 PM
**Deleted:** ,

187 the figure enclosing both Indianapolis and places that lie outside of its boundaries. This domain
188 was used for the inversion performed in Lamb et al. (2016). The second domain is Marion
189 County outlined with a green dashed line. It is assumed here that this domain is much more
190 representative of the actual Indianapolis municipal boundaries as this area encompasses the
191 majority of the urban development associated with the city of Indianapolis (Gurney et al., 2012).
192 The larger domain has three additional landfills that, based on the EPA gridded inventory
193 (Maasakkers et al., 2016), increase Indianapolis $CH_4$ emissions by about 50% when compared to
194 the smaller domain. The inversion explained in Lamb et al. (2016) has been rerun for two of the
195 domains mentioned above and the results (Fig. 1) have been reexamined.
196
197 **2.2 INFLUX tower network**
198 The continuous GHG measurements from INFLUX are described in detail in Richardson et al.
199 (2017). The measurements were made using wavelength-scanned cavity ring down
200 spectrometers (CRDS, Picarro, Inc., models G2301, G2302, G2401, and G1301), installed at the
201 base of existing communications towers, with sampling tubes secured as high as possible on each
202 tower (39 – 136 m above ground level (AGL); Miles et al., 2017). A few towers also included
203 measurements at 10 m AGL and one or two intermediate levels. While INFLUX tower in-situ
204 measurements began in September 2010, here we focus on the $CH_4$ measurements from 2013 –
205 2016. From June through December 2012, there were two or three towers with operational $CH_4$
206 measurements. By July 2013, five towers included measurements of $CH_4$, and throughout the
207 majority of the years 2015 – 2016 there were eight INFLUX towers with $CH_4$ measurements
208 (Fig. 3). Flask to in-situ comparisons and round-robin style testing indicated compatibility

209 across the tower network of 0.6 ppb $CH_4$ (Richardson et al., 2017). In this study we use hourly
210 means of $CH_4$.
211
212 **2.3 Meteorological data**
213 Wind speed and direction were measured at the Indianapolis International Airport (KIND), Eagle
214 Creek Airpark (KEYE), and Shelbyville Municipal Airport (KGEZ). The data used are hourly
215 values from the Integrated Surface Dataset (ISD) (https://www.ncdc.noaa.gov/isd) and 5-minute
216 values directly from the Automated Surface Observing System (ASOS). A complete description
217 of ASOS stations is available at https://www.weather.gov/media/asos/aum-toc.pdf. The
218 accuracy of the wind speed measurements are ±1 m/s or 5% (whichever is greater) and the
219 accuracy of the wind direction is 5 degrees when the wind speed is ≥ 2.6 m/s. The anemometers
220 are located at about 10 meters AGL. The wind data reported in ISD are given for a single point
221 in time recorded within the last 10 minutes of an hour and are closest to the value at the top of
222 the hour.
223 The planetary boundary layer height (BLH) was determined from a Doppler lidar
224 deployed in Lawrence, Indiana about 15 km to the northeast of downtown. The lidar is a Halo
225 Streamline unit, which was upgraded to have extended range capabilities in January 2016. The
226 lidar continuously performs a sequence of conical, vertical-slice, and staring scans to measure
227 profiles of the mean wind, turbulence, and relative aerosol backscatter. All of these
228 measurements are combined using a fuzzy-logic technique to automatically determine the BLH
229 continuously every 20-min (Bonin et al., 2018). The BLH is primarily determined from the
230 turbulence measurements, but the wind and aerosol profiles are also used to refine the BLH
231 estimate. The BLHs are assigned quality-control flags that can be used to identify times when

Nikolai Balashov 3/10/2020 5:25 PM
**Deleted:** data

233 the determined BLH is unreliable, such as when the air is exceptionally clean, the BLH is below
234 a minimum detectable height, or clouds and fog that attenuate the lidar signal exist. Additional
235 details about the algorithm and the lidar operation for the INFLUX project are provided in Bonin
236 et al. (2018). Doppler lidar measurements are available at
237 https://www.esrl.noaa.gov/csd/projects/influx/.
238
239 **2.4 Urban methane background**
240 Both aircraft mass balance and inverse modeling methodologies rely on an accurate estimation of
241 the urban $CH_4$ enhancement relative to the urban $CH_4$ background in order to produce a reliable
242 flux estimate (Cambaliza et al., 2014; Lamb et al., 2016). The $CH_4$ mole fraction enhancement is
243 defined as,

$$C_{enhancement} = C_{downwind} - C_{bg} \quad (1)$$

244 where $C_{downwind}$ is the $CH_4$ mole fraction measured downwind of a source and $C_{bg}$ is the $CH_4$
245 background mole fraction, which can be measured upwind of the source, but this is not
246 necessary. Background, as defined in this body of literature, is a mole fraction measurement that
247 does not contain the influence of the source of interest, but which is assumed to accurately
248 represent mole fractions that are upwind of the source of interest and measured simultaneously
249 with the downwind mole fractions.
250 Aircraft mass balance studies of Indianapolis mentioned used two main methods to
251 determine a background value. The first method calculates an average of the aircraft transect
252 edges that lie outside of the city domain (Cambaliza et al., 2014). In the second approach, a
253 horizontally varying background is introduced by linearly interpolating median background
254 values of each of the transect edges (Heimburger et al., 2017). In theory there is also a third

method that uses an upwind transect as a background field, but in the studies above it was assumed that the edges are representative of an upwind flow. In the case of an inversion, it is common to pick a tower that is located generally away from urban sources and has on average the smallest overall enhancement (Lavaux et al., 2016). Because choosing the background involves a degree of subjectivity (Heimburger et al., 2017) we consider how these choices may influence emission estimates and introduce error, both random and systematic, using data from the INFLUX tower network.

Using tower network data from November 2014 through the end of 2016, two $CH_4$ background fields are generated for the city of Indianapolis based on two different sets of criteria. The notion is based on the fact that a choice of background is currently rather arbitrary in the literature (Heimburger et al., 2017) and at every point in time it is possible to choose multiple background values that are equally acceptable for the flux estimation. In our case both approaches identify a tower suitable to serve as a background for each of the eight wind directions (N, NE, E, SE, S, SW, W, NW), where an arc of 45° represents a direction (e.g. winds from N are between 337.5° and 22.5°). Estimating background for different wind directions is implemented to more accurately represent upwind flow that is hopefully not contaminated by local sources.

Criterion 1 corresponds to a typical choice of a background in a case of tower inversion and is based on the concept that the lowest $CH_4$ mole fraction measured at any given time is not affected by the city sources and therefore is a viable approximation of the background $CH_4$ mole fractions outside of the city (Miles et al., 2017; Lauvaux et al., 2016). Given this assumption, the tower with the lowest median of the $CH_4$ enhancement distribution (calculated by assuming the lowest measurement among all towers at a given hour as a background) for each of the wind

directions over the November 2014 through December 2016 time period is chosen as a background site (Miles et al., 2017). Criterion 2 requires that the tower is outside of Marion County (outside of the city boundaries) and is not downwind of any known regional $CH_4$ source (Fig. 2). For some wind directions, there are multiple towers that could qualify as a background; we pick towers in such a manner that they are different for each criterion given a wind direction in order to calculate the error associated with the use of different but acceptable backgrounds. The towers used for both criteria and for each of the eight wind directions are displayed in Table 1. Quantifying differences between these two backgrounds allows for an opportunity to better understand the degree of uncertainty that exists in the atmospheric $CH_4$ background at Indianapolis.

To make the comparison as uniform as possible only data from 12-16 LST are utilized (all hours are inclusive) when the boundary layer is typically well-mixed (Bakwin et al., 1998). A lag 1 autocorrelation is found between 12-16 LST hours, i.e. the hourly afternoon data are correlated to the next hour, but the correlation is not significant for samples separated by two hours or more. Therefore, hours 13 and 15 LST are eliminated to satisfy the independence assumption for hourly samples. Furthermore, we make an assumption that the data satisfy steady state conditions. If the difference between consecutive hourly wind directions exceeds 30 degrees or the difference between hours 16 and 12 LST exceeds 40 degrees, the day is eliminated. Days with average wind speeds below 2 m/s are also eliminated due to slow transport across the city (the transit time from tower 1 to tower 8 is about 7 hours at a wind speed of 2 m/s).

**2.5 Frequency and bivariate polar plots**

Frequency and bivariate polar plots are used in this work to gain more knowledge regarding $CH_4$ background variability based on criteria 1 and 2, and to identify sources located within the city. To generate these polar plots, we use the *openair* package (from R programming language) created specifically for air quality data analysis (Carslaw and Ropkins, 2012). Bivariate and frequency polar plots indicate the variability of a pollutant concentration at a receptor (such as an observational tower) as a function of wind speed and wind direction, preferably measured at the location of the receptor or within several kilometers of the receptor. The frequency polar plot is generated by partitioning the $CH_4$ hourly data into the wind speed and direction bins of 1 m $s^{-1}$ and 10° respectively. To generate bivariate polar plots, wind components $u$ and $v$ are calculated for hourly $CH_4$ mole fraction values, which are fitted to a surface using a Generalized Additive Model (GAM) framework in the following way,

$$\sqrt{C} = \beta + s(u, v) + \epsilon \quad (2)$$

where $C$ is the $CH_4$ mole fraction transformed by a square root to improve model diagnostics such as a distribution of residuals, $\beta$ is mean of the response, $s$ is the isotropic smoothing function of the wind components $u$ and $v$, and $\epsilon$ is the residual. For more details on the model see Carslaw and Beevers (2013).

### 2.6 Temporal variability and approximate flux estimation

Temporal variability in urban $CH_4$ emissions may play an important role in the corresponding emissions quantification procedures. Lamb et al. (2016) suggested that such temporal variability might partially explain the differences among $CH_4$ flux estimates shown in Figure 1. If temporal variability of $CH_4$ emissions exists within the city, disagreements in the $CH_4$ flux between studies could be attributed to differences in their sampling period. Because the INFLUX tower

Nikolai Balashov 3/10/2020 5:36 PM
**Formatted:** Subscript

Nikolai Balashov 3/10/2020 5:37 PM
**Deleted:**

Nikolai Balashov 3/10/2020 5:38 PM
**Deleted:** of urban $CH_4$ emissions

data at Indianapolis contain measurements at all hours of the day over multiple years, we can utilize this dataset to better understand the temporal variability in methane emissions in the city.

We apply a simplified atmospheric boundary layer budget, not to estimate precisely the actual city emissions, but rather to evaluate temporal variability of the emissions. We begin by assuming $CH_4$ emissions $Q_a$ (mass per unit time per unit area) are not chemically active and are constant over a distance $\Delta x$ spanning a significant portion of the city. The next assumption is that a $CH_4$ plume measured downwind of the city is well mixed within a layer of depth $H$ (which is the same as BLH). We treat wind speed $u$ as constant within the layer for every hour considered. Given the above-mentioned assumptions we can write a continuity equation describing mass conservation of $CH_4$ concentration $C$ within a box in the following fashion,

$$\Delta x H \frac{\partial C}{\partial t} = \Delta x Q_a + uH(C_b - C) + \Delta x \frac{\partial H}{\partial t}(C_a - C) \quad (3)$$

where $C_b$ is the $CH_4$ concentration upwind of the city (or background), and $C_a$ is the $CH_4$ concentration above the mixed layer (Hanna et al., 1982; Arya, 1999; Hiller et al., 2014). The left hand side of the equation represents the change in $CH_4$ concentration with time, $\Delta x Q_a$ denotes a constant $CH_4$ source over the distance $\Delta x$, $uH(C_b - C)$ indicates a change of $CH_4$ concentration due to horizontal advection, and finally $\Delta x \frac{\partial H}{\partial t}(C_a - C)$ term accounts for the vertical advection and encroachment processes that result from changing BLH. By assuming steady state conditions ($\frac{\partial C}{\partial t} = 0$ and $\frac{\partial H}{\partial t} = 0$), the equation can be simplified to

$$Q_a = \frac{uH(C - C_b)}{\Delta x} \quad (4)$$

We use equation 4 to estimate hourly $CH_4$ emissions ($Q_a$) from Indianapolis (see assumptions in the paragraph below) given hourly averaged data of $H$ from the lidar positioned in the city, wind speed ($u$) from the local weather stations, and upwind ($C_b$) and downwind ($C$)

345 $CH_4$ mole fractions measured (and then converted to concentrations) at towers 1, 8, and 13
346 (depending on a wind direction) using data from heights of 40 m, 41 m, and 87 m respectively
347 (see Fig. 2).

348 The $CH_4$ concentrations are derived from $CH_4$ mole fractions by approximating average
349 molar density of dry air (in mol $m^{-3}$) within the boundary layer for every hour of the day, where
350 variability of pressure with altitude is calculated using barometric formula and it is assumed that
351 temperature decreases with altitude by 6.5 K per kilometer. The hourly surface data for pressure
352 and temperature are taken from KIND weather station. The difference between concentrations
353 $C - C_b$ is instantaneous and not lagged, where $C_b$ represents air parcel entering the city and $C$
354 represents the same air parcel exiting the city (Turnbull et al., 2015). The $CH_4$ enhancements
355 $C - C_b$ are estimated for daytime by averaging observations spanning 12-16 LST and for
356 nighttime by averaging observations spanning 20-5 LST. These time periods are based on lidar
357 estimations of when on average $H$ varies the least. The day and night were required to contain at
358 least 3 and 9 hourly $CH_4$ values respectively for averaging to occur, otherwise the day/night is
359 eliminated. Observations when $H$ is below 100 m are not used to avoid the cases when
360 measurements from towers may be above the boundary layer. In order to better achieve the
361 assumption that the boundary layer is fully mixed (especially at night), all hours with wind
362 speeds below 4 m/s are eliminated (Van De Wiel., 2012). To approximate the emissions of the
363 whole city we need to know the approximate area of the city and the distance over which the
364 plume is affected by the city $CH_4$ sources. The area of the city is about 1024 $km^2$ (the area of
365 Marion County) and the length that plume traverses when it is over the city ranges from 32 to 35
366 km depending on which downwind tower is used. We assume that $CH_4$ measurements at towers
367 8 and 13 are representative of a vertically well-mixed city plume as the towers are located

outside of the city boundaries and allow for sufficient vertical mixing to occur. For S and SW wind directions tower 8 observations are used to represent downwind conditions with background observations coming from towers 1 and 13, respectively (based on criterion 1 shown in Table 1). For W wind direction, tower 13 observations represent the downwind with background obtained from tower 1. The wind direction is required to be sustained for at least 2 hours, otherwise the data point is eliminated.

### 2.7 Indianapolis $CH_4$ sources

Only a few known $CH_4$ point sources exist within Indianapolis (Cambaliza et al., 2015; Lamb et al., 2016). The Southside Landfill (SSLF), located near the center of the city, is thought to be the largest point source in the city with emissions ranging between about 28 mol/s (inventory from Maasakkers et al. (2016), GHG reporting program, and inverse estimates from ground-based mobile sampling employed in Lamb et al. (2016)) and 45 mol/s (aircraft; Cambaliza et al. (2015)) depending on an emission estimation methodology. However, using Cambaliza et al. (2015) aircraft data and applying a different background formulation Lamb et al. (2016) found emission values of SSLF closely agreeing with 28 mol/s estimate. SSLF could account for as little as 33% (top-down from Cambaliza et al. (2015)) or as much as 63% (inventory from Maasakkers et al. (2016)) of total Marion County $CH_4$ emissions. Other city point sources are comparatively small; the wastewater treatment facility located near SSLF contributes about 3-7 mol/s (inventory from Lamb et al. (2016)), and the transmission-distribution transfer station at Panhandle Eastern Pipeline (also known as a city gate and further in this study abbreviated as PEP) is estimated to be about 1 mol/s (inventory from Lamb et al. (2016)). The remaining $CH_4$ sources, mainly from NG infrastructure leaks and livestock, are considered to be diffuse sources

Nikolai Balashov 3/11/2020 6:04 PM
**Deleted:** ,

Nikolai Balashov 3/11/2020 6:05 PM
**Deleted:** ,

Nikolai Balashov 3/10/2020 5:59 PM
**Deleted:** t

Nikolai Balashov 3/11/2020 6:05 PM
**Deleted:** ,

and are not well known. Potential sources of emissions related to NG activities include gas regulation meters, transmission and storage, distribution leaks, and Compressed Natural Gas (CNG) fleets. These diffuse NG sources account for 21-67% of the city emissions or 20 mol/s (inventory from Maasakkers et al. (2016)) to 64 mol/s (top down from Cambaliza et al. (2015)). Livestock emissions for Marion County are estimated to be around 1.5 mol/s (inventory from Maasakkers et al. (2016)). These prior studies present conflicting conclusions regarding the magnitude of the diffuse NG $CH_4$ source in Indianapolis.

Nikolai Balashov 3/11/2020 6:06 PM
**Deleted:** ,

Nikolai Balashov 3/11/2020 6:06 PM
**Deleted:** ,

Nikolai Balashov 3/11/2020 6:06 PM
**Deleted:** ,

## 3 Results and discussion

### 3.1 Inversion and city boundaries

A significant portion of $CH_4$ emissions across the U.S. can be characterized by numerous relatively large point sources scattered throughout the country rather than by broad areas of smaller enhancements (Maasakkers et al., 2016). Because of this, the total emissions for a given domain can be very sensitive to how that domain is defined. A small increase or decrease in the domain area could add or remove a large point source and significantly impact the total emissions defined within the domain.

In the case of Indianapolis, this issue became apparent when the emissions were calculated using an atmospheric inversion model (Lamb et al., 2016; Lauvaux et al., 2016). The atmospheric inversion solved for fluxes in domain 1 (Fig. 2), which significantly increased the estimated emissions in comparison with the inventory values that were gathered mainly within Marion County (domain 2). When reduced to domain 2, inverse modeling emission estimate decreases to 107 mol/s (from about 160 mol/s), which falls within an error bar of Lamb et al. (2016) inventory estimate. This difference is significant and could at least partially explain the discrepancy shown in Figure 1 between the emission values from the inventories and emission

423 results from the inverse modeling. However, even the decreased inverse modeling estimate is
424 about 91% higher than the inventories.
425 Additionally, the subject of the domain is relevant for airborne mass balance flights
426 because a priori the magnitude and variability of background plume is unknown and could be
427 easily influenced by upwind sources. The issue of background is discussed further in the next
428 section.
429
430 **3.2 Variability in $CH_4$ background**
431 Comparisons between criterion 1 and criterion 2 $CH_4$ background mole fractions as a
432 function of wind speed and direction are visualized using frequency and bivariate polar plots
433 (Fig. 4). Both backgrounds generally agree on the higher $CH_4$ originating from the SW, SE, and
434 E wind directions (Figs. 4c-f); however, the values themselves differ especially when winds are
435 from NW, SW, and SE. As background difference plots (Figs. 4g-h) indicate, there is a
436 noticeable variability between the magnitudes of the $CH_4$ backgrounds, where criterion 2, by
437 design, typically has higher background mole fractions. The background differences, at a given
438 hour, suggest that the $CH_4$ field flowing into the city is heterogeneous with differences between
439 towers ranging from 0 to over 45 ppb (Fig. 4g). Because large gradients in $CH_4$ background over
440 the city could pose challenges for flux estimations using top down methods such as inverse
441 modeling and aircraft mass balance, it is imperative to establish whether the background
442 differences vary randomly or systematically and how to choose a background to minimize these
443 errors.
444 To further understand the nature of background variability we calculate the mean,
445 standard deviation, and standard error of background hourly differences between criterion 2 and

446 criterion 1 from November 2014 to December 2016 for each of the eight wind directions
447 mentioned in Table 1. The results are shown in Figure 5. Systematic bias is evident for the SE,
448 S, SW, W, and NW wind sectors, whereas random error dominates N, NE, and E wind
449 directions. Wind directions showing statistically significant bias have mean biases ranging from
450 2 to 5 ppb, with values as large as 8 ppb falling within the range of 2 × standard error. Standard
451 deviation plot indicates potential background discrepancy that can occur on any given day, where
452 W wind direction is the least variable with 2 × standard deviation close to 20 ppb, while SE wind
453 direction is the most variable with 2 × standard deviation falling at about 50 ppb.

454 Random errors in the mole fractions of background differences (biases) are also
455 important and are a function of the length of the data record. We quantify the random error in
456 the $CH_4$ background mole fraction differences using the bootstrap method by randomly sampling
457 2 to 150 hours (small and large sample size) of the background $CH_4$ differences for each of the
458 wind directions with replacement (we make the assumption that our differences are independent
459 since we eliminated lag 1 autocorrelation from the data). This sub-sampling experiment is
460 repeated 5000 times (Efron and Tibshirani, 1986). The standard deviations of the mean
461 (standard error) of the 5000 simulated differences are calculated for each wind direction. The
462 resulting standard errors of the city $CH_4$ background differences, multiplied by 2 to represent the
463 95% confidence intervals, are shown as a function of the length of the data record in Figure 6.
464 Because random error falls as sample size grows it makes sense to assign a threshold indicating a
465 minimum number of samples needed to achieve a theoretical precision for each wind direction.

466 One way to assign a required precision would be to make sure that the standard error
467 (random error) reaches a point where it is less than Indianapolis enhancement of about 12 ppb (a
468 higher estimate of the Indianapolis enhancement from section 3.3) by a factor of 2 when

combined with a bias (Table 2). Meaning that the sum of bias and standard error must be at most 6 ppb. In this approach each wind direction would have a different threshold because of the differences in biases. For instance, given this requirement NW direction would need a random error of 1 since its bias is 5. For NW direction, this threshold would require more than 150 samples. For N direction on the other hand, where the bias is 1, the requirement is fulfilled when random error crosses 5 ppb at 74 samples. Now we consider these random and systematic errors in $CH_4$ background differences in the context of Indianapolis urban $CH_4$ emissions.

For Indianapolis, using the INFLUX network, we estimated that depending on sample size (number of hours sampled) and wind direction, background gradient across the city over 12-16 LST could vary from 0 to about 50 ppb (Fig. 5b). Given that the average afternoon $CH_4$ enhancement of the city is around 8-12 ppb (section 3.3; Fig. 7; Cambaliza et al., 2015; Miles et al., 2017), the error on the estimated emissions could easily be over 100% if the analysis does not approach the issue of background with enough sampling. A sample size of about 50 independent hours significantly decreases background uncertainty for N, NE, E, S, and W wind directions and allows for a more accurate assessment of the $CH_4$ emissions at Indianapolis. For $CH_4$ sources with a significantly larger signal than their regional background, the mentioned background variability becomes less impactful on results, but because Indianapolis is a relatively small emitter of $CH_4$, and because there are relatively large sources outside of the city, uncertainties due to background estimation are comparatively large. Our uncertainty assessment suggests that the highly variable $CH_4$ emission values of Indianapolis from aircraft mass balance calculations shown in Figure 1 are at least partially due to the variability in the urban $CH_4$ background of Indianapolis.

Nikolai Balashov 3/10/2020 6:35 PM
**Deleted:** tower

493 **3.3. Temporal variability of methane enhancements and fluxes in Indianapolis**

494 Figure 7 presents average $CH_4$ mole fraction enhancements and flux calculations
495 (equation 4) at towers 8 and 13 for years 2014, 2016, and 2013-2016 (for the detailed
496 methodology see section 2.6). The years of 2014 and 2016 are chosen for temporal comparison
497 because they do not contain major BLH data gaps. The error bars in the figure show the standard
498 error multiplied by 2 indicating 95% confidence interval of each average.

499 One of the more interesting features in Figure 7 is a day/night variability of $CH_4$
500 emissions at Indianapolis. The most prominent example of this feature is found in Figure 7c,
501 where the estimates for both years suggest that daytime emissions are approximately twice as
502 large as the emissions at night. The decrease of the $CH_4$ emissions at night also appears in tower
503 13, but the errors are too high in those estimates to make any definitive conclusions. A similar
504 urban $CH_4$ emissions diurnal variability is reported by Helfter et al. (2016) in their study of
505 GHGs for London, UK, where they attribute diurnal variation of $CH_4$ emissions to the NG
506 distribution network activities, fugitive emissions from NG appliances, and to temperature-
507 sensitive $CH_4$ emission sources of biogenic origin (such as a landfill). Taylor et al. (2018)
508 suggest that $CH_4$ emissions from landfills exhibit a diurnal cycle with higher emissions in early
509 afternoon and 30-40% lower emissions at night.

510 With regard to yearly temporal variability we are only able to compare years 2014 and
511 2016 due to limited BLH data for other years. Results from both towers suggest that
512 Indianapolis overall $CH_4$ emissions did not change significantly between 2014 and 2016.
513 Although it is important to be cautious about interpreting actual flux estimations given the
514 assumptions mentioned in section 2.6, it is interesting to note that the flux values from both
515 towers average to about 70 mol/s, which puts our value right in between inventory and inversion

Nikolai Balashov 3/10/2020 6:38 PM
**Deleted:** the

517 estimates shown in Figure 1. If we assume that SSLF emissions are generally known (GHG
518 reporting program) that would indicate that emissions from NG distribution are likely to be about
519 14 mol/s (70%) higher than what both of the inventories currently estimate but within the error
520 bars of Lamb et al. (2016)'s inventory calculation. Another possible scenario is that SSLF
521 emissions are higher than what is currently assumed. Given these complexities, uncertainty
522 regarding the exact emissions from NG distribution at Indianapolis still remains.
523
524 **3.4 Methane Sources in Indianapolis**
525 Bottom-up emission inventories have difficulty tracking changes in sources over time. Our
526 continuous tower network observations can monitor temporal and spatial variability in sources of
527 $CH_4$ in Indianapolis. To do so we employ the aforementioned bivariate polar plots to verify
528 known sources and potentially identify unknown sources across the city. We compare two time
529 periods, 2014-2015 (two full years) and 2016. Figure 8 displays bivariate polar plots of $CH_4$
530 enhancements using criterion 1 background at 9 INFLUX towers in Indianapolis over the two
531 years of 2014 and 2015. Figure 9 shows the same plot, but for the year 2016. Here we have
532 separated 2016 from 2014-2015 because of different results noted during these times.
533 The images reveal that the most consistent and strongest source in the city is the SSLF.
534 This is most evident from the 40+ ppb $CH_4$ enhancements detected at towers 7, 10 and 11
535 coming from the location of the SSLF (by triangulation). Enhancements from the landfill appear
536 to also be detectable at towers 2, 4, 5, and 13. Based on these observations it can be concluded
537 that there are no other point sources in Marion County comparable in size to the SSLF. A small
538 fraction of the SSLF plume is likely due to the co-located wastewater facility, but the inventory
539 estimates suggest that the wastewater treatment facility is responsible for no more than 7% of

this plume (Cambaliza et al., 2015; Massakkers et al., 2016). The PEP, located in the northwestern section of the city, may be partially responsible for a plume of 5-10 ppb at towers 5 and 11. However, the plume is less detectable using the criterion 2 background value that has higher background (using tower 8 as a background) from NW wind direction (not shown), adding uncertainty to the true magnitude of the enhancement from this source. The same is true for towers 2 and 13, which have pronounced plumes when winds are from the NW with the criterion 1 background, but when background 2 is used these plumes vanish (not shown). Such inconsistency makes it difficult to attribute these plumes to a specific source.

Another important point is the cluster of large enhancements surrounding tower 10 in 2014-2015. Because no other tower sees these enhancements (at least at comparable magnitudes), we believe that they are the result of nearby NG leaks. These plumes are not consistent temporally or spatially as they mostly disappear in 2016, potentially indicating that they are transient and localized NG distribution leaks. It is difficult to ascertain the exact combined magnitude of these leaks since they mix together with SSLF into an aggregated city plume when observed from downwind towers such as 8 and 13. None of the individual leaks appears to be similar in magnitude to the emissions that originate from SSLF. Diffuse NG emissions comparable to the SSLF source (Lamb et al., 2016) may exist. Our flux estimations at towers 8 and 13, however, imply that the magnitude of NG diffuse source suggested by the top-down analyses in Cambaliza et al. (2015) and Lamb et al. (2016) are probably overestimates (see section 3.3). We hypothesize that the relatively high Indianapolis $CH_4$ emissions (see Fig. 1) reported by Cambaliza et al. (2015) could be a result of random errors in upwind conditions (see section 3.2) influencing the small number of airborne flux estimates.

## 4 Conclusions

We have examined four potential contributions to discrepancies between urban top-down and bottom-up estimates of $CH_4$ emissions from Indianapolis: domain definition, heterogeneous background mole fractions, temporal variability in emissions, and sources missing from inventories. Results indicate that the urban domain definition is crucial for the comparison of the emission estimates among various methods. Our atmospheric inverse flux estimates for Marion County, which is similar to the domain that is analyzed by inventory and airborne mass balance methodologies (Mays et al., 2009; Cambaliza et al., 2014; Lamb et al., 2016), is 107 mol/s compared to 160 mol/s that is estimated for the larger domain (Hestia inventory domain; Gurney et al., 2012). This partially explains higher emissions in inverse modeling estimates shown by Lamb et al. (2016); however, 107 mol/s is still 91% higher than what EPA and Lamb et al. (2016) find in their inventories (Fig. 1).

To better understand background variability at Indianapolis two different but acceptable background estimates, based on specific criteria for each wind direction, and their differences are used to assess heterogeneity of $CH_4$ background at Indianapolis. Background criterion 1 looks for a tower that is consistently lower than other towers, while background criterion 2 picks a tower that is outside of Marion County domain and is not downwind of any nearby sources as determined by EPA 2012 inventory. We focus on midday atmospheric conditions to avoid the complexities of vertical stratification in the stable boundary layer. The midday Indianapolis atmospheric $CH_4$ mole fraction background is shown to be heterogeneous with 2-5 ppb statistically significant biases for NW, W, SW, S and SE wind directions. Random errors of background differences are a function of sample size and decrease as a number of independent samples increase. Small sample sizes, such as a few hours of data from a single point, are prone

Nikolai Balashov 3/11/2020 5:58 PM
**Deleted:** A

Nikolai Balashov 3/11/2020 6:08 PM
**Deleted:** ,

Nikolai Balashov 3/11/2020 6:09 PM
**Deleted:** ,

589 to random errors on the order of 10-30 ppb in the $CH_4$ background, similar to the magnitude of
590 the total enhancement from the city of Indianapolis, which is estimated to be on average around
591 10-12 ppb. Longer-term sampling and/or more extensive background sampling are necessary to
592 reduce the random errors. Sample size required to reduce random errors of background
593 differences to an acceptable value for flux calculation is largely dependent on a wind direction.
594 Both bias (long-term average of background differences) and its random error are important
595 when estimating total background uncertainty. The results indicate that N, NE, E, S, and W
596 wind directions are more favorable for flux estimation and would require multiple days of
597 measurements (e.g. about 50 independent hours of measurements) to reduce background
598 uncertainty to about 6 ppb, which is half the magnitude of the typical $CH_4$ enhancement from
599 Indianapolis. The remaining wind directions would require over 150 independent hourly
600 measurements to achieve similar precision. We also estimate that depending on a wind direction
601 for any given hour the spatial variability in background can be anywhere from 0 to 50 ppb. This
602 uncertainty in the $CH_4$ background may partially explain Heimburger et al. (2017) finding of
603 large variability in airborne estimates of Indianapolis $CH_4$ emissions. Given many samples, the
604 airborne studies converge to an average value of $CH_4$ flux that is noticeably closer to the
605 inventory estimates for Indianapolis than several of the individual estimates presented in Figure
606 1.

607 Measurement and analysis strategies can minimize the impacts of these sources of error.
608 Spatially extensive measurement of upwind $CH_4$ mole fractions are recommended. For towers or
609 other point-based measurements, multiple upwind measurement locations are clearly beneficial.
610 For the aircraft mass balance approach, we recommend an upwind transect to be measured,
611 lagged in time if possible, to provide a more complete understanding of the urban background

612 conditions. Complex background conditions might suggest that data from certain days or wind
613 directions should not be used for flux calculation. Finally, a mesoscale atmospheric modeling
614 system informed with the locations of important upwind $CH_4$ sources can serve as a powerful
615 complement to the atmospheric data (Barkley et al., 2017). Such simulations can guide sampling
616 strategies, and aid in interpretation of data collected with moderately complex background
617 conditions.

618 With regard to temporal variability, no statistically detectable changes in the emission
619 rates were observed when comparing 2014 and 2016 $CH_4$ emissions. However, a large
620 difference between day and night $CH_4$ emissions was implied from a simple budget estimate.
621 Night (20-5 LST) emissions may be 2 times lower than the emissions during the afternoon (12-
622 16 LST) hours. Because prior estimates of top-down citywide emissions are derived using
623 afternoon-only measurements, overall emissions of Indianapolis may be lower than these studies
624 suggest. This bias may be present in studies performed in other cities as well. Our study
625 suggests that day/night differences in $CH_4$ emissions must be understood if regional emission
626 estimates are to be calculated correctly. Long-term, tower-based observations are an effective
627 tool for understanding and quantifying multi-year variability in urban emissions.

628 One final point addressed in this study is the location of major $CH_4$ sources in
629 Indianapolis. Analysis of the INFLUX tower observations suggest a diffuse NG source that
630 exceeds both of the inventory estimates by 70%, but additionally our analysis shows that the
631 discrepancy is less than that proposed by highest values reported in Lamb et al. (2016) (see Fig.
632 1). Uncertainty remains regarding the magnitude of the diffuse NG source of $CH_4$. The only
633 major point source in the city is SSLF and it is observed at multiple towers. There is an evidence

for occasional point-source NG leaks, but they appear to be transient in time, and limited in their strength.

Overall, assessment of the $CH_4$ emissions at Indianapolis highlights a number of uncertainties that need to be considered in any serious evaluation of urban $CH_4$ emissions. These uncertainties amplify for Indianapolis since the enhancement signal from its $CH_4$ emissions is comparable in magnitude to variability in the regional background flow and as our results show it may be difficult at times to distinguish noise in the background from the actual city emissions signal. The evaluation of larger $CH_4$ sources may be easier with respect to separating signal from background. However, all of the points raised in this work will be nonetheless relevant and need to be addressed for our understanding of urban $CH_4$ emissions to significantly improve.

**Author Contribution**

Nikolay Balashov, Kenneth Davis, and Natasha Miles developed the study and worked together on generating the main hypothesis of this work. They also wrote most of the manuscript. Nikolay Balashov wrote all of the codes and performed the analyses presented in this work as well as generated all of the figures. Natasha Miles and Scott Richardson helped with maintenance and gathering of the INFLUX tower data. They also wrote section 2.2 of the paper. Thomas Lauvaux helped with the analysis presented in Fig. 1 and section 3.1 concerning interpretation of the inversion modeling results from Lamb et al. (2016). Thomas Lauvaux also helped with repeating the inversion experiment for two different Indianapolis domains (Fig. 1). Zachary Barkley significantly contributed to discussions regarding the hypothesis and careful presentation of sections 2.6 and 3.3. Timothy Bonin provided all of the lidar data and wrote the

second part of section 2.3 regarding the lidar and the methodology used to determine planetary boundary layer heights. He also contributed to sections 2.6 and 3.3.

**Competing Interests**

The authors declare that they have no conflict of interest.

**Acknowledgements**

This research has been supported by the National Institute of Standards and Technology (project number 70NANB10H245). We would like to thank Dr. Bram Maasakkers for the helpful discussion regarding the EPA 2012 inventory and the relevant error structure. We also thank Dr. Paul Shepson and Dr. Brian Lamb for their useful input regarding airborne mass balance flights and the process of compiling an emissions inventory. Most importantly, we would like to acknowledge significant contributions of both reviewers who rigorously examined our science and noticeably improved clarity of our article.

**References**

Alvarez, R. A., Zavala-Araiza, D., Lyon, D. R., Allen, D. T., Barkley, Z. R., Brandt, A. R., Davis, K. J., Herndon, S. C., Jacob, D. J., Karion, A., Kort, E. A., Lamb, B. K., Lauvaux, T., Maasakkers, J. D., Marchese, A. J., Omara, M., Pacala, S. W., Peischl, J., Robinson, A. L., Shepson, P. B., Sweeney, C., Townsend-Small, A., Wofsy, S. C., and Hamburg, S. P.: Assessment of methane emissions from the U.S. oil and gas supply chain, Science, 10.1126/science.aar7204, 2018.

Arya, S. P.: Air pollution meteorology and dispersion, Oxford University Press New York, 1999.

Barkley, Z. R., Lauvaux, T., Davis, K. J., Deng, A., Miles, N. L., Richardson, S. J., Cao, Y., Sweeney, C., Karion, A., Smith, M., Kort, E. A., Schwietzke, S., Murphy, T., Cervone, G., Martins, D., and Maasakkers, J. D.: Quantifying methane emissions from natural gas

684 production in north-eastern Pennsylvania, Atmos. Chem. Phys., 17, 13941-13966,
685 10.5194/acp-17-13941-2017, 2017.
686 Bakwin, P. S., Tans, P. P., Hurst, D. F., and Zhao, C.: Measurements of carbon dioxide on very
687 tall towers: results of the NOAA/CMDL program, Tellus, 50B, 401–415, 1998.
688 Bonin, T. A., Carroll, B. J., Hardesty, R. M., Brewer, W. A., Hajny, K., Salmon, O. E., and
689 Shepson, P. B.: Doppler lidar observations of the mixing height in Indianapolis using an
690 automated composite fuzzy logic approach, Journal of Atmospheric and Oceanic
691 Technology, 35, 473-490, 10.1175/jtech-d-17-0159.1, 2018.
692 Brandt, A. R., Heath, G. A., Kort, E. A., O'Sullivan, F., Pétron, G., Jordaan, S. M., Tans, P.,
693 Wilcox, J., Gopstein, A. M., Arent, D., Wofsy, S., Brown, N. J., Bradley, R., Stucky, G.
694 D., Eardley, D., and Harriss, R.: Methane leaks from North American natural gas
695 systems, Science, 343, 733-735, 10.1126/science.1247045, 2014.
696 Cambaliza, M., Shepson, P., Bogner, J., Caulton, D., Stirm, B., Sweeney, C., Montzka, S.,
697 Gurney, K., Spokas, K., and Salmon, O.: Quantification and source apportionment of the
698 methane emission flux from the city of Indianapolis, Elem. Sci. Anth., 3, 2015.
699 Cambaliza, M. O. L., Shepson, P. B., Caulton, D. R., Stirm, B., Samarov, D., Gurney, K. R.,
700 Turnbull, J., Davis, K. J., Possolo, A., Karion, A., Sweeney, C., Moser, B., Hendricks, A.,
701 Lauvaux, T., Mays, K., Whetstone, J., Huang, J., Razlivanov, I., Miles, N. L., and
702 Richardson, S. J.: Assessment of uncertainties of an aircraft-based mass balance approach
703 for quantifying urban greenhouse gas emissions, Atmos. Chem. Phys., 14, 9029-9050,
704 10.5194/acp-14-9029-2014, 2014.
705 Carslaw, D. C., and Ropkins, K.: openair — An R package for air quality data analysis,
706 Environmental Modelling & Software, 27-28, 52-61,
707 https://doi.org/10.1016/j.envsoft.2011.09.008, 2012.
708 Carslaw, D. C., and Beevers, S. D.: Characterising and understanding emission sources using
709 bivariate polar plots and k-means clustering, Environmental Modelling & Software, 40,
710 325-329, https://doi.org/10.1016/j.envsoft.2012.09.005, 2013.
711 Ciais, P., Sabine, C., Bala, G., Bopp, L., Brovkin, V., Canadell, J., Chhabra, A., DeFries, R.,
712 Galloway, J., and Heimann, M.: Carbon and other biogeochemical cycles, in: Working
713 Group I Contribution To The IPCC Fifth Assessment Report. Climate Change 2013 - The
714 Physical Science Basis, edited by: Stocker, T. F., Qin, D., Plattner, G., Tignor, M., Allen,

S., Boschung, J., Nauels, A., Xia, Y., Bex, V., and Midgley, P., Cambridge Univ. Press, 465-570, 2013.

Davis, K. J., Deng, A., Lauvaux, T., Miles, N. L., Richardson, S. J., Sarmiento, D. P., Gurney, K. R., Hardesty, R. M., Bonin, T. A., and Brewer, W. A.: The Indianapolis Flux Experiment (INFLUX): A test-bed for developing urban greenhouse gas emission measurements, Elem. Sci. Anth., 5, 2017.

Deng, A., Lauvaux, T., Davis, K. J., Gaudet, B. J., Miles, N., Richardson, S. J., Wu, K., Sarmiento, D. P., Hardesty, R. M., and Bonin, T. A.: Toward reduced transport errors in a high resolution urban $CO_2$ inversion system, Elem. Sci. Anth., 5, 2017.

Efron, B., and Tibshirani, R.: Bootstrap methods for standard errors, confidence intervals, and other measures of statistical accuracy, Statist. Sci., 1, 54-75, 10.1214/ss/1177013815, 1986.

European Commission Joint Research Centre, Netherlands Environmental Assessment Agency: Emission Database for Global Atmospheric Research (EDGAR), Release Version 4.2, available at: http://edgar.jrc.ec.europa.eu, 2010.

Gurney, K. R., Razlivanov, I., Song, Y., Zhou, Y., Benes, B., and Abdul-Massih, M.: Quantification of fossil fuel $CO_2$ emissions on the building/street scale for a large U.S. city, Environmental Science & Technology, 46, 12194-12202, 10.1021/es3011282, 2012.

Hanna, S. R., Briggs, G. A., and Hosker Jr, R. P.: Handbook on atmospheric diffusion, National Oceanic and Atmospheric Administration, Oak Ridge, TN (USA). Atmospheric Turbulence and Diffusion Lab., 1982.

Heimburger, A. M., Harvey, R. M., Shepson, P. B., Stirm, B. H., Gore, C., Turnbull, J., Cambaliza, M. O., Salmon, O. E., Kerlo, A.-E. M., and Lavoie, T. N.: Assessing the optimized precision of the aircraft mass balance method for measurement of urban greenhouse gas emission rates through averaging, Elem. Sci. Anth., 5, 2017.

Helfter, C., Tremper, A. H., Halios, C. H., Kotthaus, S., Bjorkegren, A., Grimmond, C. S. B., Barlow, J. F., and Nemitz, E.: Spatial and temporal variability of urban fluxes of methane, carbon monoxide and carbon dioxide above London, UK, Atmos. Chem. Phys., 16, 10543-10557, 10.5194/acp-16-10543-2016, 2016.

Hendrick, M. F., Ackley, R., Sanaie-Movahed, B., Tang, X., and Phillips, N. G.: Fugitive methane emissions from leak-prone natural gas distribution infrastructure in urban

environments, Environmental Pollution, 213, 710-716, https://doi.org/10.1016/j.envpol.2016.01.094, 2016.

Hiller, R. V., Neininger, B., Brunner, D., Gerbig, C., Bretscher, D., Künzle, T., Buchmann, N., and Eugster, W.: Aircraft-based $CH_4$ flux estimates for validation of emissions from an agriculturally dominated area in Switzerland, Journal of Geophysical Research: Atmospheres, 119, 4874-4887, doi:10.1002/2013JD020918, 2014.

Hmiel, B., Petrenko, V. V., Dyonisius, M. N., Buizer, C., Smith A. M., Place, P. F., Harth, C., Beaudette, R., Hua, Q., Yang, B., Vimont, I., Michel, S. E., Severinghaus, J. P., Etheridge, D., Bromley, Schmitt, J., Faïn, X., Weiss, R. F., and Dlugokencky, E.: Preindustrial $^{14}CH_4$ indicates greater anthropogenic fossil $CH_4$ emissions, Nature, 578, 409–412, https://doi.org/10.1038/s41586-020-1991-8, 2020.

Jackson, R. B., Down, A., Phillips, N. G., Ackley, R. C., Cook, C.W., Plata, D. L., and Zhao, K. G.: Natural gas pipeline leaks across Washington, DC, Environ. Sci. Technol., 48, 2051–2058, doi:10.1021/es404474x, 2014.

Jeong, S., Millstein, D., and Fischer, M. L.: Spatially explicit methane emissions from petroleum production and the natural gas system in California, Environmental Science & Technology, 48, 5982-5990, 10.1021/es4046692, 2014.

Jeong, S., Newman, S., Zhang, J., Andrews, A. E., Bianco, L., Bagley, J., Cui, X., Graven, H., Kim, J., Salameh, P., LaFranchi, B. W., Priest, C., Campos-Pineda, M., Novakovskaia, E., Sloop, C. D., Michelsen, H. A., Bambha, R. P., Weiss, R. F., Keeling, R., and Fischer, M. L.: Estimating methane emissions in California's urban and rural regions using multitower observations, Journal of Geophysical Research: Atmospheres, 121, 13,031-013,049, doi:10.1002/2016JD025404, 2016.

Jeong, S., Cui, X., Blake, D. R., Miller, B., Montzka, S. A., Andrews, A., Guha, A., Martien, P., Bambha, R. P., LaFranchi, B., Michelsen, H. A., Clements, C. B., Glaize, P., and Fischer, M. L.: Estimating methane emissions from biological and fossil-fuel sources in the San Francisco Bay Area, Geophysical Research Letters, 44, 486-495, doi:10.1002/2016GL071794, 2017.

Karion, A., Sweeney, C., Kort, E. A., Shepson, P. B., Brewer, A., Cambaliza, M., Conley, S. A., Davis, K., Deng, A., Hardesty, M., Herndon, S. C., Lauvaux, T., Lavoie, T., Lyon, D., Newberger, T., Pétron, G., Rella, C., Smith, M., Wolter, S., Yacovitch, T. I., and Tans,

Nikolai Balashov 3/10/2020 4:14 PM
**Formatted:** Superscript

Nikolai Balashov 3/10/2020 4:14 PM
**Formatted:** Subscript

Nikolai Balashov 3/10/2020 4:14 PM
**Formatted:** Subscript

P.: Aircraft-based estimate of total methane emissions from the Barnett Shale region, Environ. Sci. Technol., 49, 8124–8131, doi:10.1021/acs.est.5b00217, 2015

Kort, E. A., Eluszkiewicz, J., Stephens, B. B., Miller, J. B., Gerbig, C., Nehrkorn, T., Daube, B. C., Kaplan, J. O., Houweling, S., and Wofsy, S. C.: Emissions of $CH_4$ and $N_2O$ over the United States and Canada based on a receptor-oriented modeling framework and COBRA-NA atmospheric observations, Geophys. Res. Lett., 35, L18808, doi:10.1029/2008GL034031, 2008.

Lamb, B. K., Cambaliza, M. O. L., Davis, K. J., Edburg, S. L., Ferrara, T. W., Floerchinger, C., Heimburger, A. M. F., Herndon, S., Lauvaux, T., Lavoie, T., Lyon, D. R., Miles, N., Prasad, K. R., Richardson, S., Roscioli, J. R., Salmon, O. E., Shepson, P. B., Stirm, B. H., and Whetstone, J.: Direct and indirect measurements and modeling of methane emissions in Indianapolis, Indiana, Environmental Science & Technology, 50, 8910-8917, 10.1021/acs.est.6b01198, 2016.

Lauvaux, T., Miles, N. L., Deng, A., Richardson, S. J., Cambaliza, M. O., Davis, K. J., Gaudet, B., Gurney, K. R., Huang, J., O'Keefe, D., Song, Y., Karion, A., Oda, T., Patarasuk, R., Razlivanov, I., Sarmiento, D., Shepson, P., Sweeney, C., Turnbull, J., and Wu, K.: High-resolution atmospheric inversion of urban $CO_2$ emissions during the dormant season of the Indianapolis Flux Experiment (INFLUX), Journal of Geophysical Research: Atmospheres, 121, 5213-5236, doi:10.1002/2015JD024473, 2016.

Maasakkers, J. D., Jacob, D. J., Sulprizio, M. P., Turner, A. J., Weitz, M., Wirth, T., Hight, C., DeFigueiredo, M., Desai, M., Schmeltz, R., Hockstad, L., Bloom, A. A., Bowman, K. W., Jeong, S., and Fischer, M. L.: Gridded national inventory of U.S. methane emissions, Environmental Science & Technology, 50, 13123-13133, 10.1021/acs.est.6b02878, 2016.

Mays, K. L., Shepson, P. B., Stirm, B. H., Karion, A., Sweeney, C., and Gurney, K. R.: Aircraft-based measurements of the carbon footprint of Indianapolis, Environmental Science & Technology, 43, 7816-7823, 10.1021/es901326b, 2009.

McKain, K., Down, A., Raciti, S. M., Budney, J., Hutyra, L. R., Floerchinger, C., Herndon, S. C., Nehrkorn, T., Zahniser, M. S., Jackson, R. B., Phillips, N., and Wofsy, S. C.: Methane emissions from natural gas infrastructure and use in the urban region of Boston, Massachusetts, Proceedings of the National Academy of Sciences, 112, 1941-1946, 10.1073/pnas.1416261112, 2015.

Miles, N. L., Richardson, S. J., Lauvaux, T., Davis, K. J., Balashov, N. V., Deng, A., Turnbull, J. C., Sweeney, C., Gurney, K. R., and Patarasuk, R.: Quantification of urban atmospheric boundary layer greenhouse gas dry mole fraction enhancements in the dormant season: Results from the Indianapolis Flux Experiment (INFLUX), Elem. Sci. Anth., 5, 2017.

Miller, S. M., Wofsy, S. C., Michalak, A. M., Kort, E. A., Andrews, A. E., Biraud, S. C., Dlugokencky, E. J., Eluszkiewicz, J., Fischer, M. L., Janssens-Maenhout, G., Miller, B. R., Miller, J. B., Montzka, S. A., Nehrkorn, T., and Sweeney, C.: Anthropogenic emissions of methane in the United States, Proceedings of the National Academy of Sciences, 110, 20018-20022, 10.1073/pnas.1314392110, 2013.

Myhre, G., Shindell, D., Bréon, F. M., Collins, W., Fuglestvedt, J., Huang, J., Koch, D., Lamarque, J. F., Lee, D., Mendoza, B., Nakajima, T., Robock, A., Stephens, G., Takemura, T., and Zhang, H.: Anthropogenic and natural radiative forcing, in: Climate Change 2013: The Physical Science Basis. Contribution of Working Group I to the Fifth Assessment Report of the Intergovernmental Panel on Climate Change, edited by: Stocker, T. F., Qin, D., Plattner, G. K., Tignor, M., Allen, S. K., Doschung, J., Nauels, A., Xia, Y., Bex, V., and Midgley, P. M., Cambridge University Press, Cambridge, UK, 659-740, 2013.

National Academies of Sciences and Medicine: Improving characterization of anthropogenic methane emissions in the United States, The National Academies Press, Washington, DC, 250 pp., 2018.

Nisbet, E. G., Dlugokencky, E. J., Manning, M. R., Lowry, D., Fisher, R. E., France, J. L., Michel, S. E., Miller, J. B., White, J. W. C., Vaughn, B., Bousquet, P., Pyle, J. A., Warwick, N. J., Cain, M., Brownlow, R., Zazzeri, G., Lanoisellé, M., Manning, A. C., Gloor, E., Worthy, D. E. J., Brunke, E.-G., Labuschagne, C., Wolff, E. W., and Ganesan, A. L.: Rising atmospheric methane: 2007–2014 growth and isotopic shift, Global Biogeochemical Cycles, 30, 1356-1370, doi:10.1002/2016GB005406, 2016.

Nisbet, E. G., Manning, M. R., Dlugokencky, E. J., Fisher, R. E., Lowry, D., Michel, S. E., Myhre, C. L., Platt, S. M., Allen, G., Bousquet, 15 P., Brownlow, R., Cain, M., France, J. L., Hermansen, O., Hossaini, R., Jones, A. E., Levin, I., Manning, A. C., Myhre, G., Pyle, J. A., Vaughn, B. H., Warwick, N. J., and White, J. W. C.: Very Strong Atmospheric Methane Growth in the 4 Years 2014–2017: Implications for the Paris Agreement, Global

Biogeochemical Cycles, 33, 318–342, https://doi.org/10.1029/2018GB006009, https://agupubs.onlinelibrary. wiley.com/doi/abs/10.1029/2018GB006009, 2019.

Richardson, S. J., Miles, N. L., Davis, K. J., Lauvaux, T., Martins, D. K., Turnbull, J. C., McKain, K., Sweeney, C., and Cambaliza, M. O. L.: Tower measurement network of in-situ $CO_2$, $CH_4$, and CO in support of the Indianapolis FLUX (INFLUX) Experiment, Elem Sci Anth, 5, 2017.

Sarmiento, D. P., Davis, K. J., Deng, A., Lauvaux, T., Brewer, A., and Hardesty, M.: A comprehensive assessment of land surface-atmosphere interactions in a WRF/Urban modeling system for Indianapolis, IN, Elem. Sci. Anth., 5, 2017.

Saunois, M., Jackson, R. B., Bousquet, P., Poulter, B., and Canadell, J. G.: The growing role of methane in anthropogenic climate change, Environmental Research Letters, 11, 120207, 2016.

Schuh, A. E., Lauvaux, T., West, T. O., Denning, A. S., Davis, K. J., Miles, N., Richardson, S., Uliasz, M., Lokupitiya, E., Cooley, D., Andrews, A., and Ogle, S.: Evaluating atmospheric $CO_2$ inversions at multiple scales over a highly inventoried agricultural landscape, Global change biology, 19, 1424-1439, doi:10.1111/gcb.12141, 2013.

Taylor, D. M., Chow, F. K., Delkash, M., and Imhoff, P. T.: Atmospheric modeling to assess wind dependence in tracer dilution method measurements of landfill methane emissions, Waste Management, 73, 197-209, https://doi.org/10.1016/j.wasman.2017.10.036, 2018.

Townsend-Small, A., Tyler, S. C., Pataki, D. E., Xu, X., and Christensen, L. E.: Isotopic measurements of atmospheric methane in Los Angeles, California, USA: Influence of "fugitive" fossil fuel emissions, J. Geophys. Res.-Atmos., 117, 1–11, https://doi.org/10.1029/2011JD016826, 2012.

Turnbull, J. C., Sweeney, C., Karion, A., Newberger, T., Lehman, S. J., Tans, P. P., Davis, K. J., Lauvaux, T., Miles, N. L., Richardson, S. J., Cambaliza, M. O., Shepson, P. B., Gurney, K., Patarasuk, R., and Razlivanov, I.: Toward quantification and source sector identification of fossil fuel $CO_2$ emissions from an urban area: Results from the INFLUX experiment, Journal of Geophysical Research: Atmospheres, 120, 292-312, doi:10.1002/2014JD022555, 2015.

Turnbull, J. C., Karion, A., Davis, K. J., Lauvaux, T., Miles, N. L., Richardson, S. J., Sweeney, C., McKain K., Lehman, S. J., Gurney, K., Patarasuk, R., Jianming L., Shepson, P. B.,

Heimburger A., Harvey, R., and Whetstone, J.: Synthesis of urban $CO_2$ emission estimates from multiple methods from the Indianapolis Flux Project (INFLUX), Environmental Science and Technology, 53 (1), 287-295, 10.1021/acs.est.8b05552, 2019.

U.S. Environmental Protection Agency: Inventory of U.S. Greenhouse Gas Emissions and Sinks: 1990–2011, Technical Report EPA 430-R-13-001, Environmental Protection Agency, Washington, 505 pp., 2013.

Van De Wiel, B. J. H. V. d., Moene, A. F., Jonker, H. J. J., Baas, P., Basu, S., Donda, J. M. M., Sun, J., and Holtslag, A. A. M.: The minimum wind speed for sustainable turbulence in the nocturnal boundary layer, Journal of the Atmospheric Sciences, 69, 3116-3127, 10.1175/jas-d-12-0107.1, 2012.

Wunch, D., Wennberg, P. O., Toon, G. C., Keppel-Aleks, G., and Yavin, Y. G.: Emissions of greenhouse gases from a North American megacity, Geophysical Research Letters, 36, doi:10.1029/2009GL039825, 2009.

Zavala-Araiza, D., Lyon, D. R., Alvarez, R. A., Davis, K. J., Harriss, R., Herndon, S. C., Karion, A., Kort, E. A., Lamb, B. K., Lan, X., Marchese, A. J., Pacala, S. W., Robinson, A. L., Shepson, P. B., Sweeney, C., Talbot, R., Townsend-Small, A., Yacovitch, T. I., Zimmerle, D. J., and Hamburg, S. P.: Reconciling divergent estimates of oil and gas methane emissions, Proceedings of the National Academy of Sciences, 112, 15597-15602, 10.1073/pnas.1522126112, 2015.

## Tables

**Table 1.** INFLUX towers used to estimate $CH_4$ background based on two different criteria. Numbers in bold indicate towers chosen to generate a background field when multiple options are possible (for more details see discussion). In short, criterion 1 uses towers with the lowest mean $CH_4$ for a specific wind direction, and criterion 2 uses towers outside of Marion County and not downwind of large sources (including the city as a whole).

| Wind Direction | $CH_4$ Background Towers | |
|---|---|---|
| | Criterion 1 | Criterion 2 |
| North (N) | 8 | **13**, 8 |
| Northeast (NE) | 8 | **13**, 8, 2 |
| East (E) | **2**, 8 | **8**, 4, 1, 2 |
| Southeast (SE) | 1 | **8**, 13, 4, 1 |
| South (S) | 1 | **4**, 13, 1 |
| Southwest (SW) | 13 | **1**, 4 |
| West (W) | 1 | **4**, 1 |
| Northwest (NW) | 1 | **8**, 1 |

**Table 2.** A number of independent samples needed (column 4) to satisfy combined requirement of 6 ppb background error based on the sum of bias and random error (explained in section 3.2) as a function of wind direction.

| Wind Direction | Bias (ppb) | Threshold (ppb) | Samples Needed |
|---|---|---|---|
| N | 1 | 5 | 74 |
| NE | 1 | 5 | 36 |
| E | 0.5 | 5.5 | 46 |
| SE | 4 | 2 | >150 |
| S | 2 | 4 | 53 |
| SW | 4.5 | 1.5 | >150 |
| W | 3 | 3 | 52 |
| NW | 5 | 1 | >150 |

961
962 **Figures**
963

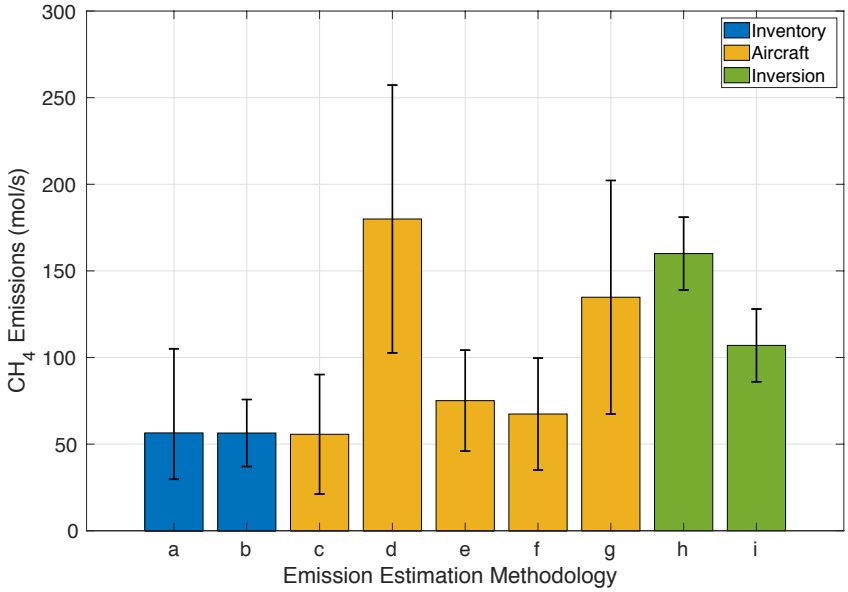


964

965 **Figure 1.** Various estimates of $CH_4$ emissions at Indianapolis. **(a, b)** Bottom-up estimates of $CH_4$
966 emissions conducted by Lamb et al. (2016) in 2013 and Maasakkers et al. (2016) based on the EPA 2012
967 inventory respectively. Error bars show 95% confidence intervals (for more details see above-mentioned
968 articles). **(c-g)** Top-down evaluations of $CH_4$ emissions with aircraft from various flight campaigns where
969 **(c)** contains 5 flights over March-April of 2008, **(d)** contains 3 flights over November-January of 2008-
970 09, **(e)** contains 5 flights over April-July of 2011, **(f)** contains 9 flights from November-December, 2014,
971 and **(g)** contains the same 5 flights over April-July of 2011 as in (e) but uses different methodology.
972 Methodologies for **(c-f)** are described in Lamb et al. (2016) and methodology for **(g)** is described in
973 Cambaliza et al. (2015). Error bars show 95% confidence intervals (for more details see above-
974 mentioned articles). **(h, i)** Top-down evaluations of $CH_4$ emissions for 2012-2013 using tower inversion
975 modeling methodology with two different domains, where **(h)** uses the full domain of Figure 2 and **(i)**
976 uses only the Marion County domain of Figure 2. The inversion methodology and 95% confidence
977 intervals are described in detail in Lamb et al. (2016).

978
979
980
981

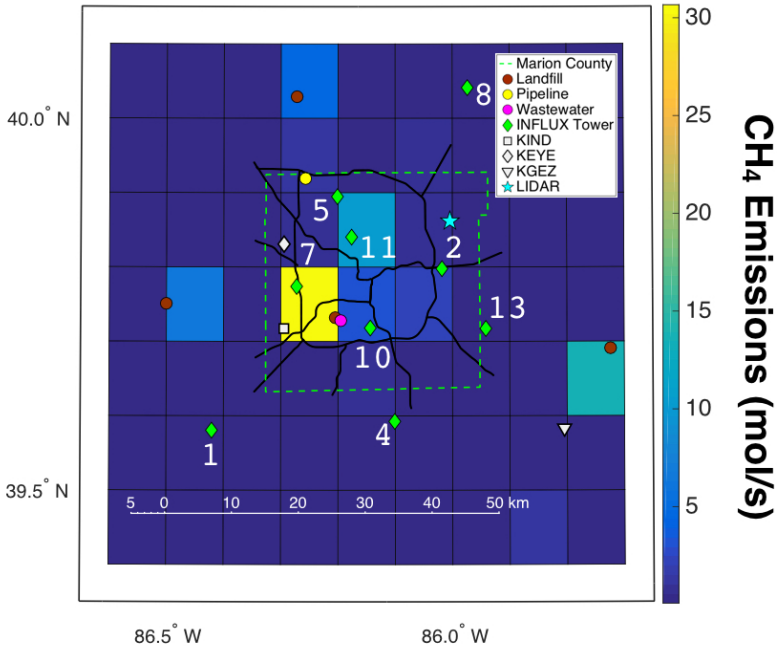


982

983 **Figure 2.** Map of the primary roads in Indianapolis, INFLUX towers, lidar system, weather stations, and
984 a few $CH_4$ point sources plotted over the gridded $CH_4$ emissions (mol/s) from the EPA 2012 Inventory
985 (Maasakkers et al., 2016). The gridded map of emissions includes emissions from the mentioned point
986 sources; their position is provided to aid in interpretation of the observations. The dashed bright green
987 line denotes Marion County borders.

988

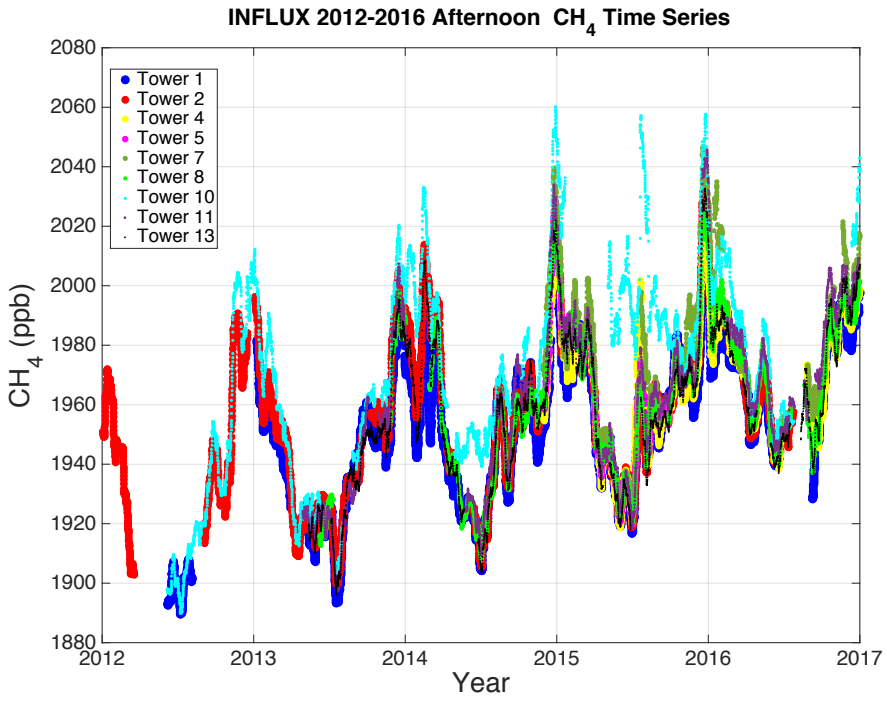


989

990 **Figure 3.** 20-day running average of afternoon (12-16 LST; the hours are inclusive) $CH_4$ mole fractions
991 as measured by the INFLUX tower network (highest available height is used) from 2012 through 2016.

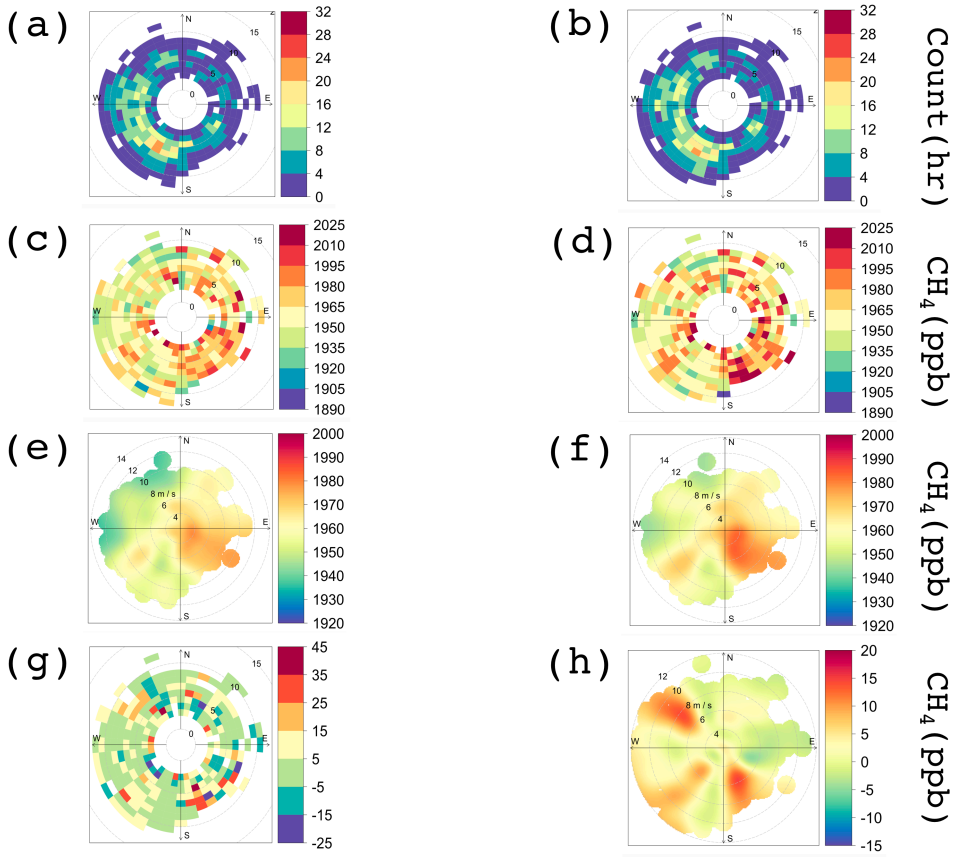


**Figure 4.** Frequency and bivariate polar plots of $CH_4$ background for Indianapolis using data from 12-16 LST, November 2014 through December 2016 given 2 different criteria (Table 1). **(a)** Polar histogram indicating a number of hourly measurements available using criterion 1. **(b)** Same as (a) only for criterion 2. Differences between (a) and (b) are due to slight differences in data availability at the considered towers. **(c)** Polar frequency plot of the $CH_4$ background using criterion 1. **(d)** Same as (c) only for criterion 2. **(e)** Polar bivariate plot of $CH_4$ background using criterion 1. **(f)** Same as (e) only for criterion 2. **(g)** Polar frequency plot of difference between the backgrounds: $criterion\ 2 - criterion\ 1$. **(h)** Same as (g) but shown with a bivariate polar plot.

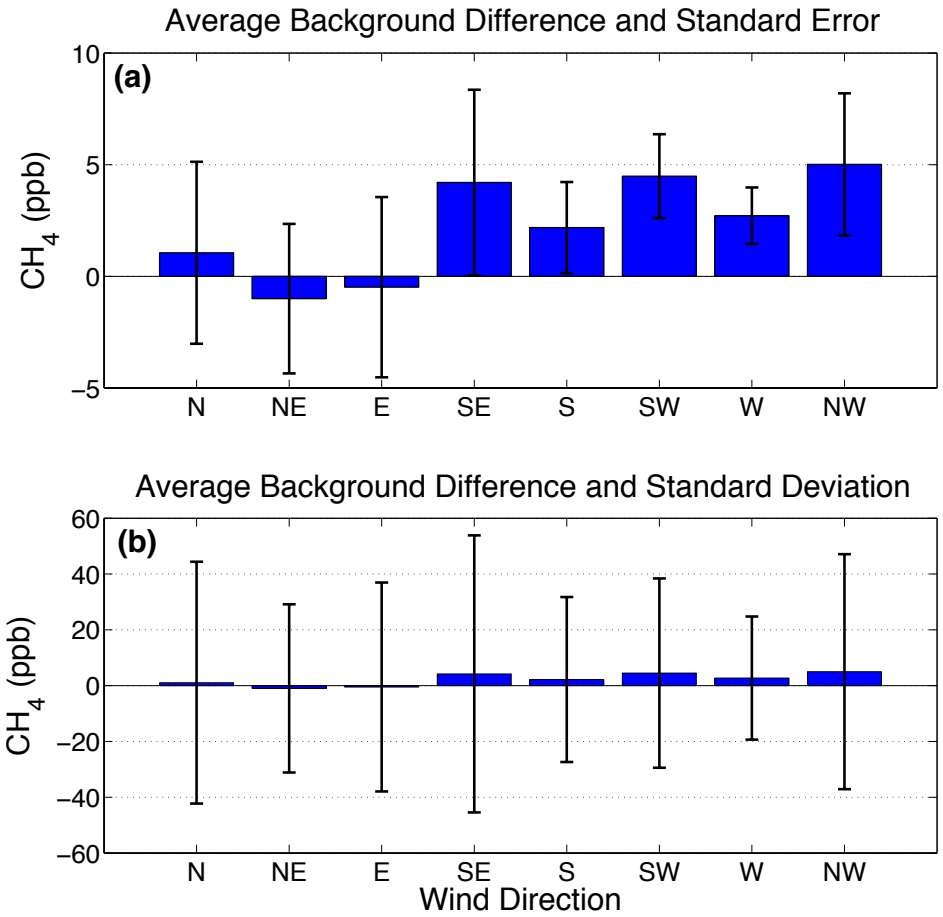


**Figure 5.** Average of the differences between criteria 2 and 1 $CH_4$ backgrounds at Indianapolis as a function of wind direction. These averages are generated from the same data that is used in Figure 4 and reflect results shown in Figure 4g. Error bars indicate in **(a)** 2 × standard error and in **(b)** 2 × standard deviation.

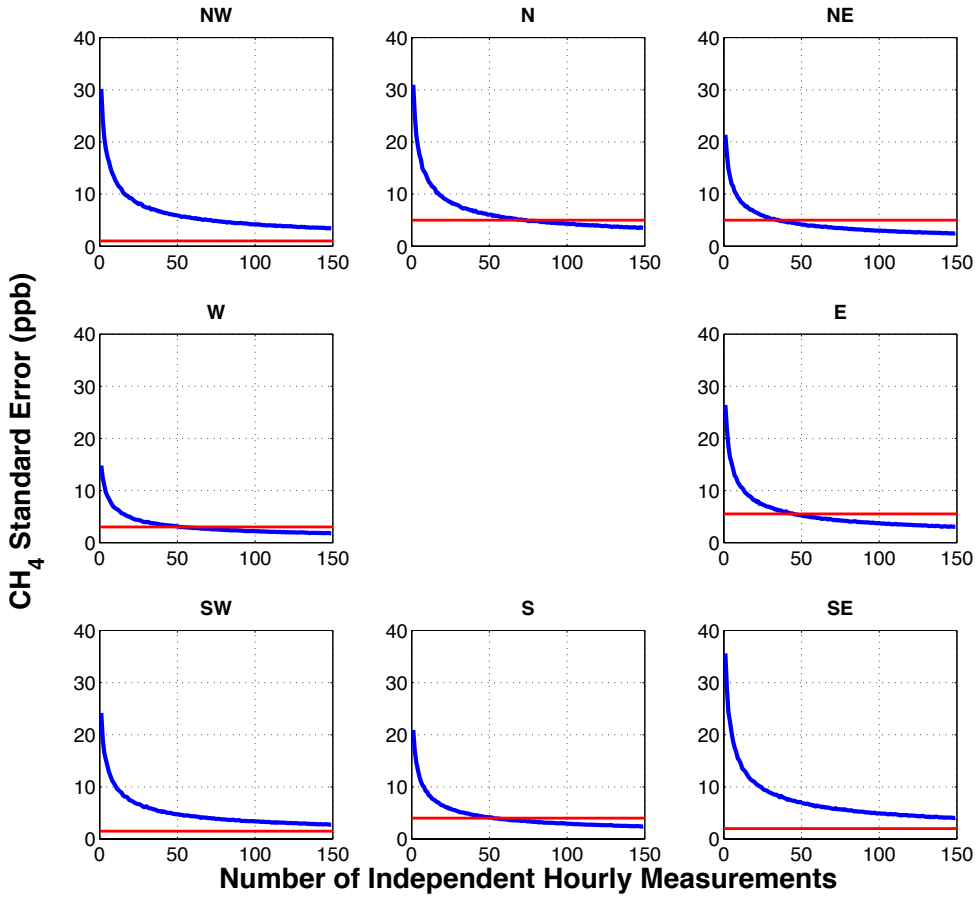


**Figure 6.** Bootstrap simulation of the standard errors × 2 in Indianapolis $CH_4$ background mole fraction differences (between criteria 2 and 1) as a function of sample size and wind direction (see text for details). Thresholds for each of the wind directions indicate a random error threshold needed for the background uncertainty to be within 50% of Indianapolis $CH_4$ enhancement of 12 ppb.

1013

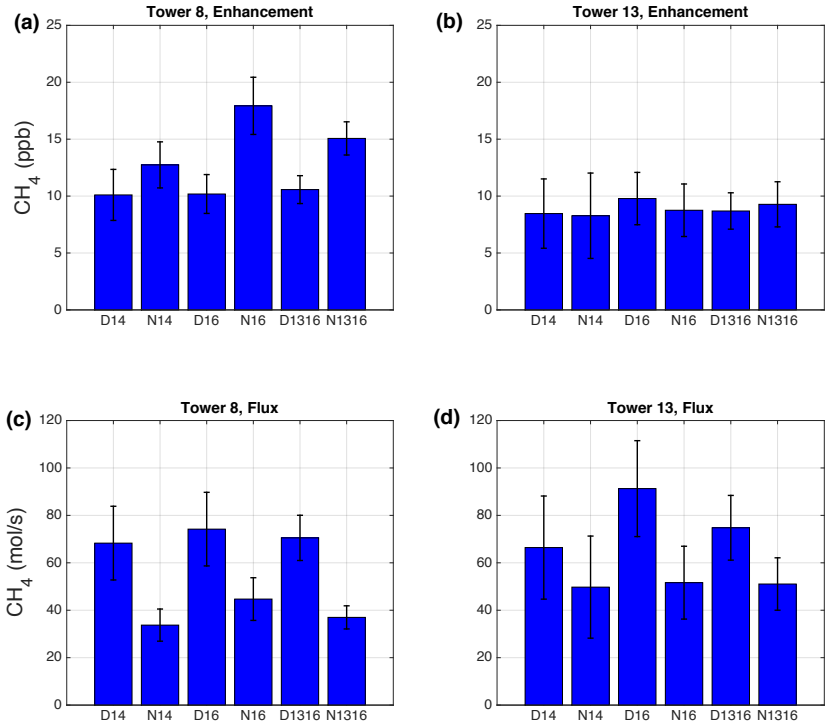


1014

1015 **Figure 7.** Averages of the daytime (D) and nighttime (N) $CH_4$ enhancements and fluxes at INFLUX
1016 towers 8 and 13 for years 2014 (14), 2016 (16), and 2013-2016 (1316). The error bars represent 95%
1017 confidence interval of each mean value. **(a)** Estimates of $CH_4$ enhancements from tower 8. **(b)** Estimates
1018 of $CH_4$ enhancements from tower 13. **(c)** Estimates of $CH_4$ flux from tower 8. **(d)** Estimates of $CH_4$ flux
1019 from tower 13.

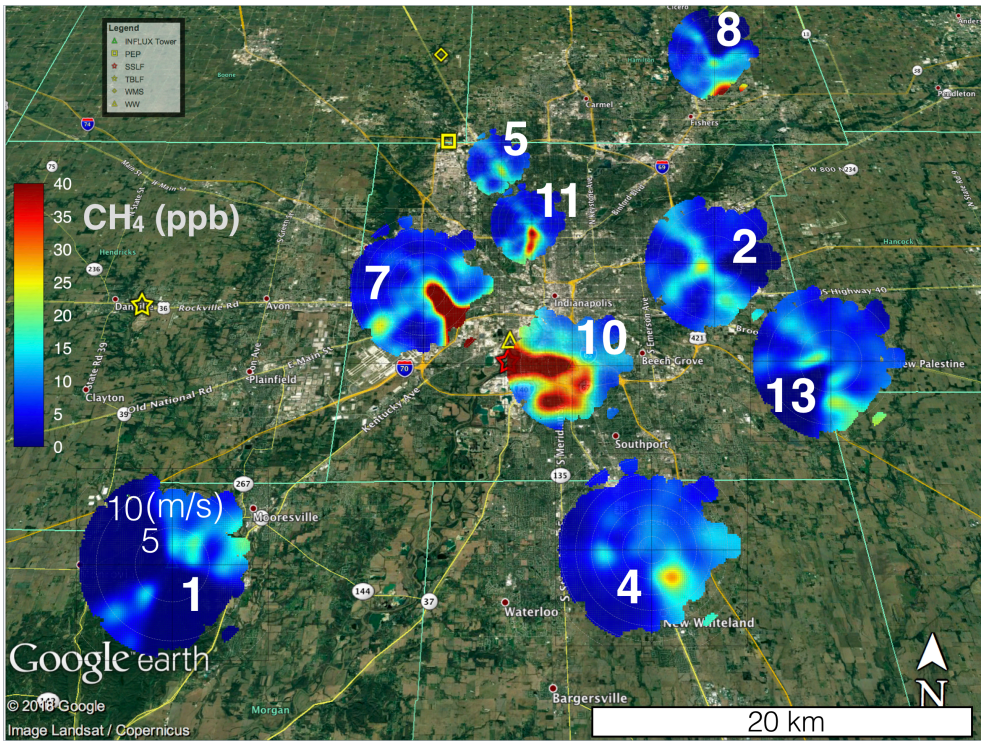


**Figure 8.** Google Earth image overlaid with bivariate polar plots (section 2.5) of the $CH_4$ enhancements at 9 INFLUX towers in Indianapolis using the criterion 1 background (Table 1) for full years of 2014 and 2015 over the afternoon (12-16 LST). The wind speed scale is only labeled at site 1; other sites follow the same convention. Legend indicates known sources of $CH_4$: Panhandle Eastern Pipeline (PEP), Southern Side Landfill (SSLF), Twin Bridges Landfill (TBLF), Waste Management Solutions (WMS), and Waste Water treatment facility (WW). The known magnitudes of sources that are in Marion County (PEP, SSLF, and WW) are reported in section 2.7. Magnitudes of TBLF and WMS according to EPA are approximately 5 mol/s. The largest known source on the map is SSLF.

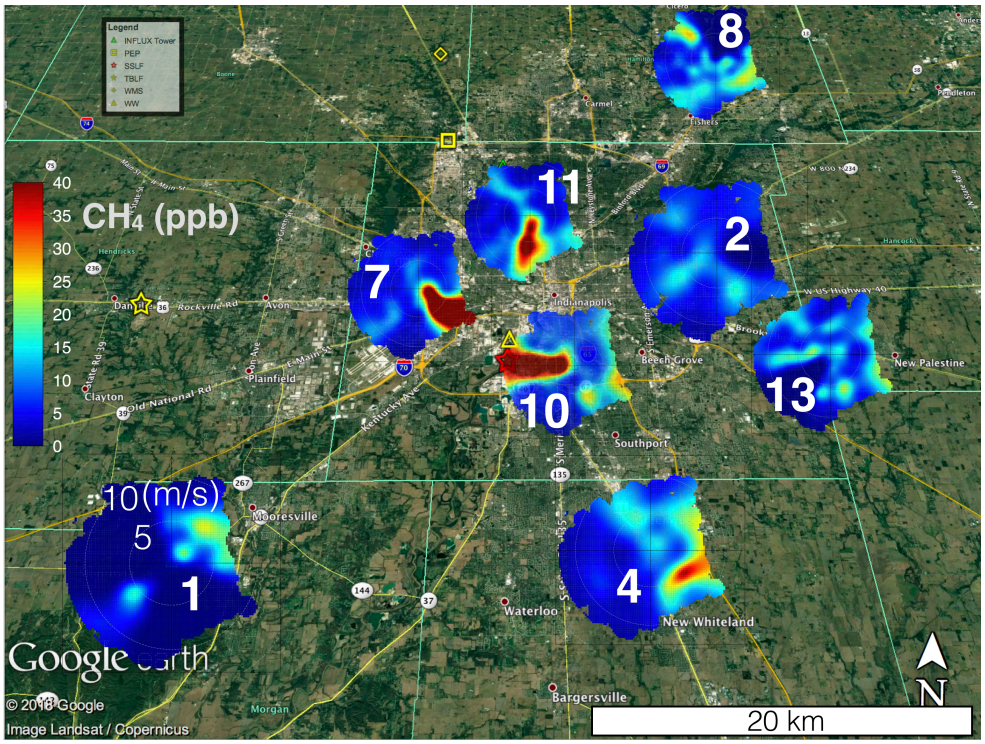


**Figure 9.** Google Earth image overlaid with bivariate polar plots (section 2.5) of the $CH_4$ enhancements at 9 INFLUX towers in Indianapolis using the criterion 1 background (Table 1) for year 2016 over the afternoon (12-16 LST). The wind speed scale is only labeled at site 1; other sites follow the same convention. Legend indicates known sources of $CH_4$: Panhandle Eastern Pipeline (PEP), Southern Side Landfill (SSLF), Twin Bridges Landfill (TBLF), Waste Management Solutions (WMS), and Waste Water treatment facility (WW). The known magnitudes of sources that are in Marion County (PEP, SSLF, and WW) are reported in section 2.7. Magnitudes of TBLF and WMS according to EPA are approximately 5 mol/s. The largest known source on the map is SSLF.